openheart

Cardiovascular MR T2-STIR imaging does not discriminate between intramyocardial haemorrhage and microvascular obstruction during the subacute phase of a reperfused myocardial infarction

Esben Søvsø Szocska Hansen,[1,2] Steen Fjord Pedersen,[3] Steen Bønløkke Pedersen,[4] Uffe Kjærgaard,[1] Nikolaj Hjort Schmidt,[5] Hans Erik Bøtker,[6] Won Yong Kim[1,6]

To cite: Hansen ESS, Pedersen SF, Pedersen SB, *et al*. Cardiovascular MR T2-STIR imaging does not discriminate between intramyocardial haemorrhage and microvascular obstruction during the subacute phase of a reperfused myocardial infarction. *Open Heart* 2016;**3**:e000346. doi:10.1136/openhrt-2015-000346

ESSH and SFP contributed equally.

Received 6 October 2015
Revised 24 February 2016
Accepted 29 March 2016

For numbered affiliations see end of article.

Correspondence to
Esben Søvsø Szocska Hansen;
esben@clin.au.dk

ABSTRACT

Objective: Microvascular obstruction (MVO) and intramyocardial haemorrhage (IMH) are known complications of myocardial ischaemia-reperfusion injury. Whereas MVO is an established marker for a poor clinical outcome, the clinical significance of IMH remains less well defined. Cardiovascular MR (CMR) and T2 weighted short tau inversion recovery (T2-STIR) imaging have been used to detect IMH and to explore its clinical importance. IMH is typically identified within the area-at-risk as a hypointense signal core on T2-STIR images. Because MVO will also appear as a hypointense signal core, T2-STIR imaging may not be an optimal method for assessing IMH. In this study, we sought to investigate the ability of T2-STIR to discriminate between MVO with IMH in a porcine myocardial ischaemia-reperfusion model that expressed MVO with and without IMH.

Method: MVO with and without IMH (defined from both macroscopic evaluation and T1 weighted CMR) was produced in 13 pigs by a 65-min balloon occlusion of the mid left anterior descending artery, followed by reperfusion. Eight days after injury, all pigs underwent CMR imaging and subsequently the hearts were assessed by gross pathology.

Results: CMR identified MVO in all hearts. CMR and pathology showed that IMH was present in 6 of 13 (46%) infarcts. The sensitivity and specificity of T2-STIR hypointense signal core for identification of IMH was 100% and 29%, respectively. T2-values between hypointense signal core in the pigs with and without IMH were similar (60.4±3 ms vs 63.0±4 ms).

Conclusions: T2-STIR did not allow identification of IMH in areas with MVO in a porcine model of myocardial ischaemic/reperfusion injury in the subacute phase of a reperfused myocardial infarction.

KEY QUESTIONS

What is already known about this subject?

- Cardiovascular MR (CMR) using T2 weighted imaging with short tau inversion recovery (T2-STIR) is being used to detect microvascular obstruction (MVO) with intramyocardial haemorrhage (IMH) as markers of myocardial ischaemia-reperfusion. However, the validity of T2 weighted CMR in assessment of IMH has not been tested.

What does this study add?

- In this study, we find that T2-STIR does not discriminate between MVO and IMH in an experimental model of myocardial ischaemia-reperfusion that expresses MVO with and without IMH during the subacute phase of a reperfused myocardial infarction.

How might this impact on clinical practice?

- A comprehensive multicontrast CMR protocol is needed to evaluate the presence of MVO and IMH in acute myocardial infarction.

INTRODUCTION

Timely reperfusion is mandatory to salvage ischaemic myocardium and to reduce mortality in acute myocardial infarction.[1] Reperfusion following prolonged ischaemia may, however, injure the myocardial microvasculature and cause microvascular obstruction (MVO).[2] This is a serious condition because it prevents adequate myocardial blood perfusion despite patent coronary arteries. Severe myocardial microvascular injury may also trigger intramyocardial haemorrhage (IMH) due to extravasation of erythrocytes through the damaged endothelial wall.[3–8] Whereas MVO is recognised as a strong predictor of ventricular remodelling and poor clinical outcome, it remains

unknown whether IMH further aggravates the clinical outcome.[9] To determine the clinical consequences of IMH, it is essential to develop a reliable, non-invasive imaging technique capable of differentiating between MVO, and MVO with IMH.[10 11] Cardiovascular MR (CMR) utilises first-pass perfusion imaging and T2-weighted images to detect MVO and IMH. Specifically, T2 weighted short tau inversion recovery (T2-STIR) imaging was applied to detect IMH[6 7] and to investigate the prognostic value of IMH defined from T2-STIR.[6 7 12 13] Within the area-at-risk (AAR), usually identified by T2-weighted imaging as oedema, a hypointense core on T2-STIR images has been ascribed to paramagnetic effects of haemoglobin breakdown products, and has consequently been considered indicative of IMH.[14 15] However, because MVO consists of non-oedematous tissue, a hypointense signal core within the AAR may not be specific for IMH.[16] MVO and IMH represent two separate pathologies but often appear simultaneously since IMH is highly associated with MVO.[16] We investigated the ability of T2-STIR imaging to detect IMH and to discriminate between IMH and MVO using a unique porcine model of myocardial ischaemia-reperfusion that expresses MVO and MVO with IMH.[17]

METHODS

Animal model

Fifteen female Danish Landrace pigs each weighing ~40 kg were used for the experiments. The pigs were presedated with an intramuscular injection of Stressnil (1 mL/kg) and midazolam (1 mL/kg). After induction of anaesthesia with intravenous propofol (3.33 mg/kg) and endotracheal intubation, anaesthesia was maintained with sevoflurane (2.5%) and continuous rate infusion of fentanyl (3 mg/kg/h). The pigs were mechanically ventilated with a tidal volume of 425 mL (12 ventilations/min). By ultrasound guidance, an 8 F introducer sheath was inserted into the right common femoral artery. This was followed by an intravenous bolus injection of heparin (100 IU/kg). Coronary occlusion was induced by placing a 2.5 mm angioplasty balloon in the left anterior descending coronary artery (LAD) distal to the second diagonal branch artery and inflating it to 10 atm. The balloon occluded the LAD for 65 min, and was then deflated and removed. A coronary angiogram was performed following balloon inflation, to confirm occlusion, and also following balloon deflation, to confirm reperfusion. The animals were randomised to receive either intracoronary infusion of saline or dimethyl sulfoxide during reperfusion as a potential adjunctive therapy to reduce reperfusion injury. The details of the experimental protocol are described elsewhere.[17]

During the procedure, heart rate, ECG, blood pressure, temperature and oxygen saturation were continuously monitored. Ampicillin (2 mg) was administrated intravenously before and after the procedure, and acetylsalicylic acid (100 mg/day) was given orally after the procedure and continued until euthanasia. To prevent ventricular fibrillation, 150 mg of amiodarone was administered intravenously prior to the induction of myocardial infarction. If ventricular fibrillation was encountered, non-synchronised direct current defibrillation (150 J) was performed. The paddles were pressed against the anterior chest wall above the sternum on the right side and below the sternum on the left side. At the end of the experiment, the pigs were awakened and returned to their stables, where they stayed for 7–10 days (average 8.5 days) prior to CMR imaging, harvesting and evaluation by gross pathology.

CMR imaging

All the pigs underwent CMR imaging before euthanasia. The sedation protocol was as described above, except that continuous propofol infusion (10 mg/mL, 12 mL/h) was used instead of sevoflurane. CMR was performed on a 1.5 T MR system (Intera, Philips Medical Systems, Best, the Netherlands) with a five-element cardiac synergy coil. All images of the heart were obtained with the pigs in the supine position. First, a survey scan was performed to localise the heart and diaphragm, and then left ventricular (LV) function was assessed using a retrospective, ECG-triggered Balanced-Steady-State-Free-Precession (B-SSFP) breath-hold cine sequence in the cardiac short-axis, vertical long axis and horizontal long axis planes. In the cardiac short-axis, the LV volume was completely encompassed by contiguous 8 mm slices with a spatial resolution of 1.22×1.22 mm and a field of view (FOV) of 288×288 mm. The following imaging parameters were used: repetition time (TR) 3.0 ms; echo time (TE) 1.5 ms; flip angle 60°; 30 heart phases. To ensure a strong T2-weighting, a T2-STIR fast spin echo sequence with a long TE was obtained in the previously mentioned short-axis orientation to assess AAR. The sequence was navigator-gated and cardiac-triggered. The following imaging parameters were used: TR 2400 ms; TE 100 ms; echo train length 20; fat inversion time 180 ms; flip angle 90°; spatial resolution 0.54 mm×0.54 mm in-plane; number of averages 2; slice thickness 8 mm; FOV 320×320 mm; 14 slices.

We obtained T2-mapping in six animals by a multislice spin echo sequence. The sequence was navigator-gated and cardiac-triggered. The following imaging parameters were used: TR 1100 ms; TE (8, 16, 24, 32, 40, 48, 56, 64) ms; flip angle 90°; spatial resolution 1.33×1.33 mm in-plane; slice thickness 8 mm; FOV 320×320 mm; 14 slices.

T1-weighted inversion recovery (T1W-IR) gradient echo (GRE) imaging was obtained in the same short-axis slices for the purpose of identifying IMH, as previously described.[18] The sequence was navigator-gated, free-breathing and cardiac-triggered. The following imaging parameters were used: TR 3.5 ms; TE 1.13 ms; flip angle 30°; spatial resolution 1×1 mm in-plane; slice thickness

8 mm (over contiguous slices); FOV 320×320 mm and 14 slices. Before the acquisition of the T1W IR sequence, a TI scout (Look Locker sequence) was performed for the purpose of obtaining the most appropriated TI to null the signal intensity from blood. Typically, the TI was found to be optimal at approximately 500 ms.

Subsequently, gadolinium enhanced first-pass myocardial perfusion and late gadolinium enhancement (LGE) was performed for the purpose of identifying areas of MVO and myocardial infarction, respectively. An intravenous bolus dose of 0.2 mmol/kg Gd-DTPA (Gadobutrol, Gadovist, Bayer Schering Pharma, Berlin, Germany) was administered manually. First-pass perfusion imaging was performed using a fast gradient echo sequence with the following parameters: TR 2.5 ms; TE 1.3 ms; flip angle 18°; spatial resolution 2.8×3.0 mm in-plane; slice thickness 10 mm; FOV 256×256 mm; three slices acquired in the LV short-axis using a 5 mm interslice gap.

LGE was acquired 15 min after gadolinium injection, using a three-dimensional phase sensitive inversion recovery-prepared T1-weighted gradient echo sequence with the following parameters: TR 5.78 ms; TE 2.78 ms; echo train length 20; inversion time ~320 ms; flip angle 25°; spatial resolution 1.5×1.5 mm; slice thickness 8 mm; FOV 350×350 mm; 14 slices acquired in the LV short-axis with no interslice gap. Following CMR, the pigs were kept under anaesthesia and moved to the operating room for organ harvesting.

Harvesting and pathology

Midline sternotomy was performed and a snare placed around the LAD distal to the second diagonal branch at the same site as the previous balloon occlusion. Twenty-five millilitres of 10% Evans blue dye was then injected into the left auricle and allowed to circulate for approximately 10 s, to delineate the AAR.[18–20] The animal was subsequently euthanised and the heart excised. The heart was then cut into consecutive 8 mm-thick slices in short-axis planes. Each slice was photographed with a digital camera (Nikon, Tokyo, Japan) for the purpose of registering myocardial infarction, IMH and AAR.

DATA ANALYSIS

CMR images

One observer (WYK), blinded to the distribution of the groups, analysed all the CMR images, using the semiautomatic, freely available software Segment V.1.9 R3697. First, LV volumes and function were calculated on the end-diastolic and end-systolic phases of the short-axis cine images. Second, myocardial infarct size was determined in the LGE images by a semiautomated algorithm accounting for partial volume effects.[21] The infarct size was expressed as a percentage of the LV myocardium (infarction volume/LV myocardium volume×100%). The AAR was quantified from T2-STIR images by a semiautomated algorithm (AAR/LV myocardium volume×100%).[22] The salvaged myocardial percentage was defined as the difference between the infarct size and AAR. Finally, the hypointense signal core within the AAR was defined by ROI analysis as a core with signal intensity measuring two SDs lower than the signal intensity of the AAR.[23 24] The ROI defined by the hypointense signal core was used on the T2-mapping images to extract T2 values. On the T1W IR images, myocardium with mean signal intensity more than two SDs above the mean signal intensity from remote myocardium was defined as IMH (18). MVO was defined and quantified on the LGE images from visual inspection of no contrast enhancement within the infarct core. All CMR images were matched and aligned.

Pathology

Two observers by consensus (SFP and ESSH) analysed all photographed gross pathological images of the myocardial slices using the Adobe Photoshop software (Adobe Systems Inc, San Jose, California, USA). The IMH volume was identified and measured as a distinct red to reddish black area within the AAR of the LV myocardium. MVO was not assessed in the pathology.

Statistics

The significance of group differences was evaluated using the Mann-Whitney U test and the Wilcoxon matched-pairs signed rank test was used to evaluate the amount of IMH in percentage of the left ventricle on T1W IR images compared to gross pathology. Data are presented as mean and 95% CIs. A value of $p<0.05$ was considered statistically significant. The association between IMH and MVO, and presence of hypointense signal core on T2-STIR images, was tested with a 2-tailed Fisher's exact test. T2-mapping values were tested using a one-way analysis of variance with Holm-Sidak's multiple comparisons correction. Statistical analysis was performed with GraphPad Prism (6.05, GraphPad Software, La Jolla, California, USA).

RESULTS

All CMR examinations and experimental procedures were successfully completed. Figure 1 shows representative pathological photographs and CMR images of MVO (−IMH) and MVO (+IMH). Examples from gross pathology assessment are shown in figure 2. The CMR and gross pathology results are summarised in table 1. Two pigs displayed neither MVO nor IMH. Global CMR parameters did not show any significant difference in ejection fraction or LV volumes between the two groups. AAR, infarct size and myocardial salvage also did not show any difference between the groups. The MVO size measured as a percentage of LV on LGE images showed no difference in the MVO (+IMH) group compared with the MVO (−IMH) group, 2.1% vs 1.7%, respectively. The sensitivity and specificity of T2-STIR hypointense signal core to detect IMH was 100% and 29%, respectively, as

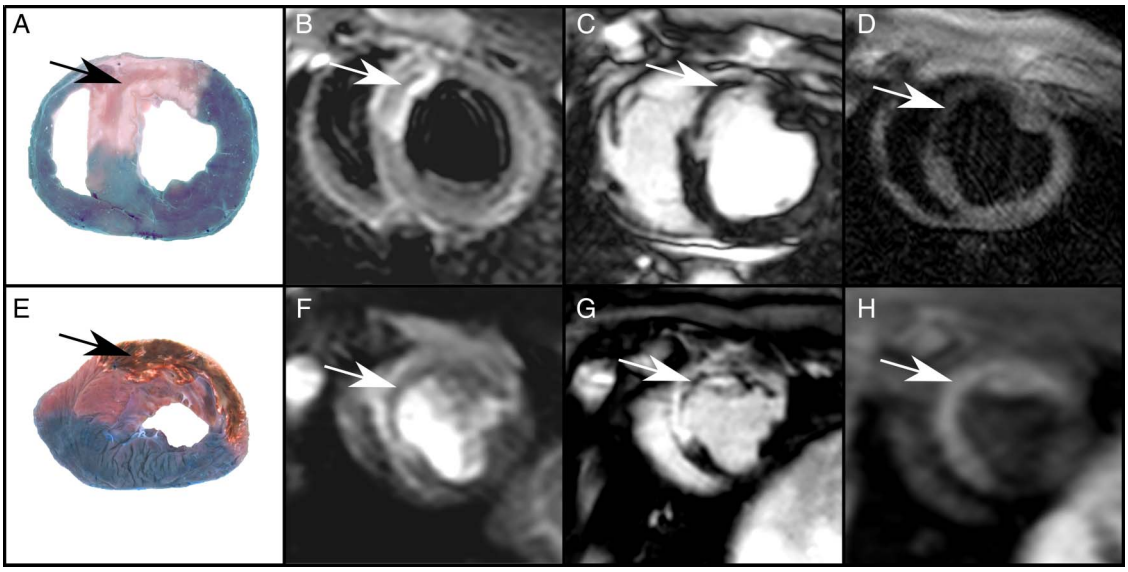

Figure 1 Upper row shows myocardial infarction with MVO (−IMH) (indicated by arrows) on pathology (A), T2-STIR (B), late gadolinium enhancement (LGE) images (C) and T1W IR (D). Lower row shows myocardial infarction with MVO (+IMH) (indicated by arrows) on pathology (E), T2-STIR (F) and LGE images (G), and T1W IR (H). IMH, intramyocardial haemorrhage; MVO, microvascular obstruction; T2-STIR, T2 weighted short tau inversion recovery.

shown in table 2. T1W IR showed that 0 out of 7 (0%) had IMH in the MVO (−IMH) group compared with 6 of 6 (100%) pigs in MVO (+IMH) group ($p<0.01$). Wilcoxon matched-pairs signed rank test showed no difference between the IMH % LV measured on T1W IR (range 12–39% LV) compared with gross pathology (range 5–27% LV) ($p=0.09$, difference 6.4% LV, CI (−2.86 to 15.76), median 5.1%, Q1=2.1, Q3=10.6).

The measured T2-values are visualised in figure 3. The T2-values (n=7) from hypointense signal core in MVO

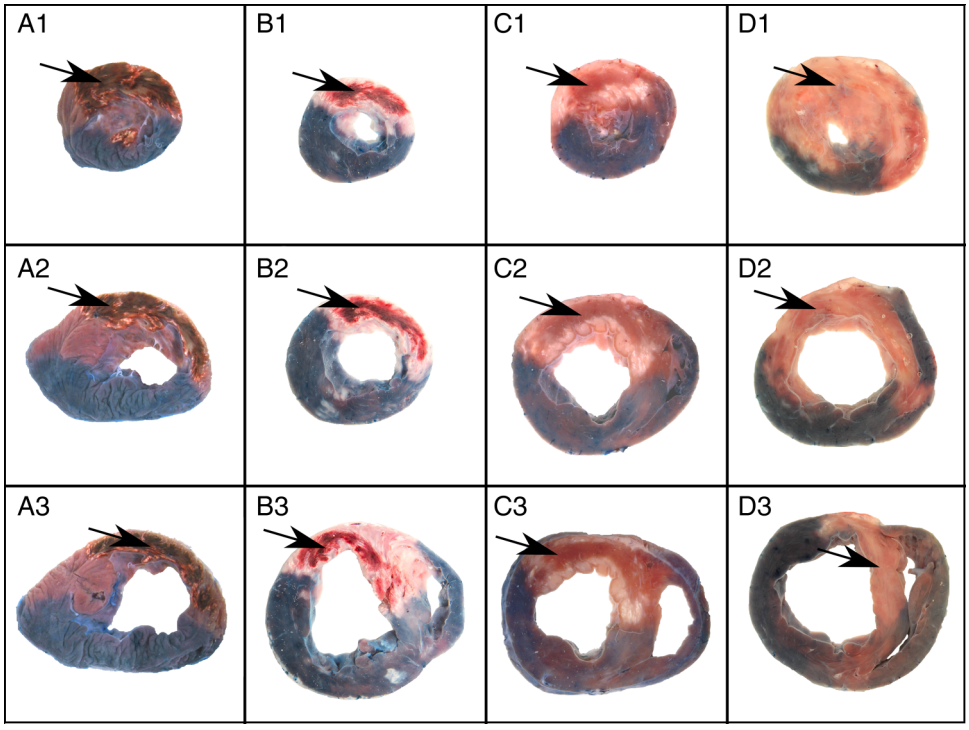

Figure 2 Examples from gross anatomical pathology. A (1–3) and B (1–3) show three slices from two pigs in the MVO (+IMH) group, where the arrows indicated areas defined as IMH. C (1–3) and D (1–3) show three slices from two pigs in the MVO (−IMH) group, where arrows points to the AAR where there is no indication of IMH. AAR, area-at-risk; IMH, intramyocardial haemorrhage; MVO, microvascular obstruction.

Table 1 Results of CMR and gross pathology

	MVO (+IMH) n=6	MVO (−IMH) n=7	Difference	p Value
Pathology results				
Number of animals with IMH (count)	6	0	–	–
CMR results				
LV end-diastolic volume (mL)	101.8	91.6	10.2 (−20.77 to 41.1)	0.34
LV end-systolic volume (mL)	48.5	45.5	3.08 (−25.2 to 31.3)	0.62
LV ejection fraction (%)	51.2	36.3	14.8 (−32.2 to 2.54)	0.10
AAR size (% LV)	37.0	36.7	0.30 (−12.8 to 13.5)	0.84
LGE infarct size (% LV)	23.0	19.7	3.32 (−5.19 to 11.8)	0.73
Myocardial salvage (% of LV)	14.0	17.0	−3.01 (−11.3 to 5.25)	0.44
MVO (n)	6	7	–	–
MVO size (% of LV)	2.2	1.7	−0.45 (−1.6 to −0.73)	0.42
T1W IR IMH (n)	6	0		<0.01
T2-STIR hypointense signal core (n)	6	5	–	–

AAR, area-at-risk; IMH, intramyocardial haemorrhage; LV, left ventricular; MVO, microvascular obstruction; T2-STIR, T2 weighted short tau inversion recovery.

(−IMH) (mean 63.0 ms) and hypointense signal core in MVO (+IMH) (mean 60.4 ms) showed no difference (p=0.9, difference −2.57 ms, CI (−9.76 to 4.61)). In the MVO (−IMH) infarcts, the T2-values from remote myocardium (mean 58.3 ms) and the hypointense signal core (mean 63.0 ms) also showed no difference (p=0.9, difference 4.60 ms, CI (−3.66 to 12.9)). Also, in the MVO (+IMH) infarcts, the T2-values from the remote myocardium (mean 58.0 ms) and the hypointense signal core (mean 60.4 ms) showed no difference (p=0.9, difference 2.35 ms, CI (−1.96 to 6.65)). Significant differences in T2-values between infarcted myocardium versus remote, hypointense signal core and salvaged myocardium, are listed in table 3.

DISCUSSION

The results of this study showed that, within the AAR, a hypointense signal core on T2-STIR images may represent IMH as well as MVO, leaving the specificity for IMH insufficient. No difference was found in T2-values within the hypointense signal core between MVO (−IMH) and MVO (+IMH). Furthermore, no difference was detected in T2 values between hypointense signal core and remote myocardium. This finding illustrates the challenge of defining AAR by T2-weighted sequences during the subacute phase in the presence of reperfusion injury. Gross pathology confirmed our T1W IR CMR findings by showing a perfect match between the two in terms of identifying IMH. In a postmortem study, Jackowski et *al*[25] previously showed that hypointense signal core on T2-STIR images might represent pathologies other than IMH, for example, non-oedematous myocardial tissue; nevertheless, we believe that this study is the first to confirm this assumption by validating the results of T2-STIR imaging against gross pathology in a subacute porcine model of reperfusion injury. In another

Table 2 Sensitivity and specificity of T2-STIR for detection of IMH

T2-STIR (±Hypointense signal core) vs MVO (±IMH)	MVO (+IMH)	MVO (−IMH)
T2-STIR (+hypointense signal core)	6	5
T2-STIR (−hypointense signal core)	0	2
Sensitivity=100%	Specificity=29%	p=0.46

IMH, intramyocardial haemorrhage; MVO, microvascular obstruction; T2-STIR, T2 weighted short tau inversion recovery.

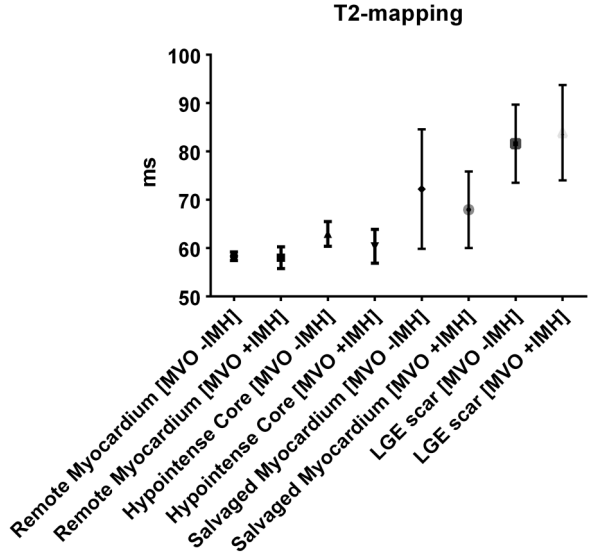

Figure 3 The mean T2-values with SDs are shown for each location of interest from both groups. IMH, intramyocardial haemorrhage; LGE, late gadolinium enhancement; MVO, microvascular obstruction.

Table 3 Comparison of T2-values from left ventricular myocardium

T2-values (ms)	Mean 1	Mean 2	Difference	p Value
Remote myocardium (MVO −IMH) vs LGE scar (MVO +IMH)	58.3	84.0	25.6	0.006
Remote myocardium (MVO +IMH) vs LGE scar (MVO −IMH)	58.0	81.6	23.6	0.01
Remote myocardium (MVO +IMH) vs LGE scar (MVO +IMH)	58.0	84.0	25.9	0.0002
Hypointense core (MVO −IMH) vs LGE scar (MVO +IMH)	63.0	84.0	21.0	0.03
Hypointense core (MVO +IMH) vs LGE scar (MVO −IMH)	60	81.6	21.3	0.03
Hypointense core (MVO +IMH) vs LGE scar (MVO +IMH)	60	84.0	23.5	0.0007
Salvaged myocardium (MVO +IMH) vs LGE scar (MVO +IMH)	68	84.0	15.96	0.03

IMH, intramyocardial haemorrhage; LGE, late gadolinium enhancement; MVO, microvascular obstruction.

experimental study, a porcine model of IMH demonstrated a correlation between hypointense signal core on T2-STIR images and histopathologically confirmed IMH.[7] In contrast to our study, the porcine model expressed only MVO with IMH. Consequently, the ability of CMR T2-STIR to differentiate between IMH and MVO could not be addressed. Several previous studies have used T2-STIR to detect IMH in patients with acute myocardial infarction for the purpose of exploring its clinical consequences.[6 12 13 23 26–30] In light of the present results, a comprehensive multicontrast CMR protocol is preferable for evaluation of the clinical consequences of IMH. To increase the accuracy of CMR IMH detection, a multisequence approach with T2*-weighted or T1-weighted sequences has been proposed in addition to T2-STIR.[31–33] The T2*-weighted sequences are very sensitive to paramagnetic effects from haemoglobin degradation products, and may be more specific for IMH. However, such sequences are time-consuming, provide negative contrast resulting in signal void and may consequently be vulnerable to motion artefacts. T1-weighted sequences take advantage of the very short T1-relaxation of methaemoglobin, and detect methaemoglobin with positive contrast, which optimises differentiation of IMH from adjacent normal myocardium.[18] Since T1-weighted sequences depend on the haemoglobin breakdown product at the methaemoglobin stage, it is only useful in the subacute phase (>7 days).[34]

LIMITATIONS

MVO was only assessed by CMR. Future studies using thioflavin-S staining might be a possible method to identify the MVO zones by pathological examination.[35] The presence of IMH on gross pathology was based on visual assessment. Histological analysis of IMH was not carried out due to suboptimal preservation of the hearts. However, the presence of IMH was also demonstrated with T1W IR performed in the subacute phase, which has been demonstrated to be a reliable marker of haemorrhage containing methemoglobin.[36] Indeed, we found a perfect agreement between gross pathology and T1W IR on determining the presence of IMH. The presence of IMH in reperfused acute ischaemic myocardium is most likely a continuum of extravasation of minute to large amounts of erythrocytes through severely damaged endothelial cells. Thus, neither visual inspection nor T1W IR CMR may have detected smaller amounts of IHM. Since the optimal time to visualise AAR from myocardial oedema is either acute or after 1 week, it is possible that imaging as late as 10 days postinfarction will result in reduced amounts of oedema within the AAR.

CONCLUSION

T2-weighted CMR, when performed in the subacute phase, does not allow discrimination between MVO with and without IMH as defined by macroscopic evaluation and T1W IR CMR. A comprehensive multicontrast CMR protocol is needed to evaluate reperfusion-induced IMH in acute myocardial infarction.

Author affiliations
[1]The MR Research Centre, Aarhus University Hospital Skejby, Aarhus N, Denmark
[2]Danish Diabetes Academy, Odense, Denmark
[3]Department of Cardiothoracic and Vascular Surgery T, Aarhus University Hospital Skejby, Aarhus N, Denmark
[4]Department of Endocrinology and Internal Medicine, Aarhus University Hospital THG, Aarhus C, Denmark
[5]Department of Clinical Medicine—Comparative Medicine Laboratory, Aarhus University Hospital Skejby, Aarhus N, Denmark
[6]Department of Cardiology, Aarhus University Hospital Skejby, Aarhus N, Denmark

Contributors ESSH took part in formulating the study design, carried out the CMR scans, contributed with work on the animal model, performed analysis of the CMR and pathology data, performed the statistical analysis and wrote the manuscript with feedback from the co-authors. SFP carried out all the procedures related to the animal model, took part in formulating the study design and drafting of the manuscript, and revised it critically for intellectual content. SBP took part in formulating the study design and drafting of the manuscript, and revised it critically and contributed to important intellectual content of the manuscript. UK contributed to procedures related to the animal model and drafting of the manuscript, and revised it critically for intellectual content. NHS contributed to procedures related to the animal model and drafting of the manuscript, and revised it critically for intellectual content. HEB took part in formulating the study design and drafting of the manuscript, and revised it critically and contributed to important intellectual content of the manuscript. WYK took part in formulating the study design and the CMR sequence setup, analysed the CMR data, contributed towards drafting of the manuscript, and revised it critically and contributed to important intellectual content of the manuscript. All the authors have read and approved the final manuscript.

Funding This work was supported by the Danish Council for Strategic Research (11-115818) and (10-093499), and by a research grant from the Danish Diabetes Academy, supported by the Novo Nordisk Foundation.

Competing interests None declared.

Provenance and peer review Not commissioned; externally peer reviewed.

Data sharing statement No additional data are available.

REFERENCES

1. Maroko PR, Libby P, Ginks WR, *et al*. Coronary artery reperfusion. I. Early effects on local myocardial function and the extent of myocardial necrosis. *J Clin Invest* 1972;51:2710–16.
2. Matsumura K, Jeremy RW, Schaper J, *et al*. Progression of myocardial necrosis during reperfusion of ischemic myocardium. *Circulation* 1998;97:795–804.
3. Basso C, Thiene G. The pathophysiology of myocardial reperfusion: a pathologist's perspective. *Heart* 2006;92:1559–62.
4. Reffelmann T, Kloner RA. The no-reflow phenomenon: a basic mechanism of myocardial ischemia and reperfusion. *Basic Res Cardiol* 2006;101:359–72.
5. Kloner RA, Ganote CE, Jennings RB. The "no-reflow" phenomenon after temporary coronary occlusion in the dog. *J Clin Invest* 1974;54:1496–508.
6. Beek AM, Nijveldt R, van Rossum AC. Intramyocardial hemorrhage and microvascular obstruction after primary percutaneous coronary intervention. *Int J Cardiovasc Imaging* 2010;26:49–55.
7. Robbers LF, Eerenberg ES, Teunissen PF, *et al*. Magnetic resonance imaging-defined areas of microvascular obstruction after acute myocardial infarction represent microvascular destruction and haemorrhage. *Eur Heart J* 2013;34:2346–53.
8. Payne AR, Berry C, Kellman P, *et al*. Bright-blood T(2)-weighted MRI has high diagnostic accuracy for myocardial hemorrhage in myocardial infarction: a preclinical validation study in swine. *Circ Cardiovasc Imaging* 2011;4:738–45.
9. Betgem RP, de Waard GA, Nijveldt R, *et al*. Intramyocardial haemorrhage after acute myocardial infarction. *Nat Rev Cardiol* 2015;12:156–67.
10. Calvieri C, Masselli G, Monti R, *et al*. Intramyocardial hemorrhage: an enigma for cardiac MRI? *BioMed Res Int* 2015;2015:859073.
11. Hamirani YS, Wong A, Kramer CM, *et al*. Effect of microvascular obstruction and intramyocardial hemorrhage by CMR on LV remodeling and outcomes after myocardial infarction: a systematic review and meta-analysis. *JACC Cardiovasc Imaging* 2014;7:940–52.
12. Eitel I, Kubusch K, Strohm O, *et al*. Prognostic value and determinants of a hypointense infarct core in T2-weighted cardiac magnetic resonance in acute reperfused ST-elevation-myocardial infarction. *Circ Cardiovasc Imaging* 2011;4:354–62.
13. Husser O, Monmeneu JV, Sanchis J, *et al*. Cardiovascular magnetic resonance-derived intramyocardial hemorrhage after STEMI: Influence on long-term prognosis, adverse left ventricular remodeling and relationship with microvascular obstruction. *Int J Cardiol* 2013;167:2047–54.
14. Lotan CS, Bouchard A, Cranney GB, *et al*. Assessment of postreperfusion myocardial hemorrhage using proton NMR imaging at 1.5 T. *Circulation* 1992;86:1018–25.
15. Lotan CS, Miller SK, Bouchard A, *et al*. Detection of intramyocardial hemorrhage using high-field proton (1H) nuclear magnetic resonance imaging. *Cathet Cardiovasc Diagn* 1990;20:205–11.
16. Ye YX, Basse-Lüsebrink TC, Arias-Loza PA, *et al*. Monitoring of monocyte recruitment in reperfused myocardial infarction with intramyocardial hemorrhage and microvascular obstruction by combined fluorine 19 and proton cardiac magnetic resonance imaging. *Circulation* 2013;128:1878–88.
17. Pedersen SF, Grøndal AK, Andersen NP, *et al*. Dimethyl sulfoxide reduces microvascular obstruction and intramyocardial hemorrhagein a Porcine ischemia-reperfusion model. *Heart Res Open J* 2015;2:85–91.
18. Pedersen SF, Thrysøe SA, Robich MP, *et al*. Assessment of intramyocardial hemorrhage by T1-weighted cardiovascular magnetic resonance in reperfused acute myocardial infarction. *J Cardiovasc Magn Reson* 2012;14:59.
19. Nakamura K, Al-Ruzzeh S, Gray C, *et al*. Effect of myocardial reperfusion on the release of nitric oxide after regional ischemia: an experimental model of beating-heart surgery. *Tex Heart Inst J* 2006;33:35–9.
20. Redfors B, Shao Y, Omerovic E. Myocardial infarct size and area at risk assessment in mice. *Exp Clin Cardiol* 2012;17:268–72.
21. Heiberg E, Ugander M, Engblom H, *et al*. Automated quantification of myocardial infarction from MR images by accounting for partial volume effects: animal, phantom, and human study. *Radiology* 2008;246:581–8.
22. Sjögren J, Ubachs JF, Engblom H, *et al*. Semi-automatic segmentation of myocardium at risk in T2-weighted cardiovascular magnetic resonance. *J Cardiovasc Magn Reson* 2012;14:10.
23. O h-Ici D, Ridgway JP, Kuehne T, *et al*. Cardiovascular magnetic resonance of myocardial edema using a short inversion time inversion recovery (STIR) black-blood technique: Diagnostic accuracy of visual and semi-quantitative assessment. *J Cardiovasc Magn Reson* 2012;14:22.
24. Croisille P, Kim HW, Kim RJ. Controversies in cardiovascular MR imaging: T2-weighted imaging should not be used to delineate the area at risk in ischemic myocardial injury. *Radiology* 2012;265:12–22.
25. Jackowski C, Christe A, Sonnenschein M, *et al*. Postmortem unenhanced magnetic resonance imaging of myocardial infarction in correlation to histological infarction age characterization. *Eur Heart J* 2006;27:2459–67.
26. Kali A, Tang RL, Kumar A, *et al*. Detection of acute reperfusion myocardial hemorrhage with cardiac MR imaging: T2 versus T2. *Radiology* 2013;269:387–95.
27. Mather AN, Fairbairn TA, Ball SG, *et al*. Reperfusion haemorrhage as determined by cardiovascular MRI is a predictor of adverse left ventricular remodelling and markers of late arrhythmic risk. *Heart* 2011;97:453–9.
28. Weaver JC, Ramsay DD, Rees D, *et al*. Dynamic changes in ST segment resolution after myocardial infarction and the association with microvascular injury on cardiac Magnetic Resonance Imaging. *Heart Lung Circ* 2011;20:111–18.
29. Amabile N, Jacquier A, Shuhab A, *et al*. Incidence, predictors, and prognostic value of intramyocardial hemorrhage lesions in ST elevation myocardial infarction. *Catheter Cardiovasc Interv* 2012;79:1101–8.
30. Wright J, Adriaenssens T, Dymarkowski S, *et al*. Quantification of myocardial area at risk with T2-weighted CMR: comparison with contrast-enhanced CMR and coronary angiography. *JACC Cardiovasc Imaging* 2009;2:825–31.
31. Kidambi A, Biglands JD, Higgins DM, *et al*. Susceptibility-weighted cardiovascular magnetic resonance in comparison to T2 and T2 star imaging for detection of intramyocardial hemorrhage following acute myocardial infarction at 3 Tesla. *J Cardiovasc Magn Reson* 2014;16:86.
32. Kidambi A, Mather AN, Motwani M, *et al*. The effect of microvascular obstruction and intramyocardial hemorrhage on contractile recovery in reperfused myocardial infarction: insights from cardiovascular magnetic resonance. *J Cardiovasc Magn Reson* 2013;15:58.
33. Kandler D, Lücke C, Grothoff M, *et al*. The relation between hypointense core, microvascular obstruction and intramyocardial haemorrhage in acute reperfused myocardial infarction assessed by cardiac magnetic resonance imaging. *Eur Radiol* 2014;24:3277–88.
34. Habs M, Pfefferkorn T, Cyran CC, *et al*. Age determination of vessel wall hematoma in spontaneous cervical artery dissection: a multi-sequence 3T cardiovascular magnetic resonance study. *J Cardiovasc Magn Reson* 2011;13:76.
35. Wu KC, Kim RJ, Bluemke DA, *et al*. Quantification and time course of microvascular obstruction by contrast-enhanced echocardiography and magnetic resonance imaging following acute myocardial infarction and reperfusion. *J Am Coll Cardiol* 1998;32:1756–64.
36. Moody AR, Murphy RE, Morgan PS, *et al*. Characterization of complicated carotid plaque with magnetic resonance direct thrombus imaging in patients with cerebral ischemia. *Circulation* 2003;107:3047–52.